Title: Geomagnetically Induced Currents in a Power Grid of northeastern Spain

J. Miquel Torta

Observatori de l'Ebre, (OE), CSIC - Universitat Ramon Llull, Horta Alta 38, E-43520 Roquetes, Spain (jmtorta@obsebre.es)

Lluís Serrano

Observatori de l'Ebre, (OE), CSIC - Universitat Ramon Llull, Horta Alta 38, E-43520 Roquetes, Spain (llserrano@obsebre.es)

J. Ramon Regué

Research Group in Electromagnetism and Communications (GRECO), La Salle, Universitat Ramon Llull (URL), Quatre Camins 30, E-08022 Barcelona, Spain (jramon@salle.url.edu)

Albert M. Sánchez

Research Group in Electromagnetism and Communications (GRECO), La Salle, Universitat Ramon Llull (URL), Quatre Camins 30, E-08022 Barcelona, Spain (albertm@salle.url.edu)

Elionor Roldán

Endesa Distribución Eléctrica S.L., Av. Paral·lel, 51, E-08004 Barcelona, Spain (elionor.roldan@endesa.es)

Citation: Torta, J. M., L. Serrano, J. R. Regué, A. M. Sánchez, and E. Roldán (2012), Geomagnetically induced currents in a power grid of northeastern Spain, Space Weather, 10, S06002, doi:10.1029/2012SW000793. To view the published open abstract, go to http://dx.doi.org and enter the DOI.

Abstract

Using the geomagnetic records of Ebro geomagnetic observatory and taking the plane wave assumption for the external current source and a homogeneous Earth conductivity, a prediction of the effects of the geomagnetic activity on the Catalonian (northeastern Spain) power transmission system has been developed. Although the area is located at mid-latitudes, determination of the geoelectric field on the occasion of the largest geomagnetic storms during the last solar cycles indicates amplitudes which are higher than those recorded in Southern Africa, where some transformer failures on large transmission systems have been reported. A DC network model of the grid has been constructed and the geomagnetically induced current (GIC) flows in the power network have been calculated for such extreme events using the electric field at Ebro as a regional proxy. In addition, GICs have been measured at one transformer neutral earthing of the power grid, so that there the accuracy of the model has been assessed. Although the agreement is quite satisfactory, results indicate that better knowledge of the ground conductivity structure is needed. This represents the first attempt to study and measure GICs in Southern European power grids, a region considered to have low GIC-risk up to the present.

Citation: Torta, J. M., L. Serrano, J. R. Regué, A. M. Sánchez, and E. Roldán (2012), Geomagnetically induced currents in a power grid of northeastern Spain, Space Weather, 10, S06002, doi:10.1029/2012SW000793. To view the published open abstract, go to http://dx.doi.org and enter the DOI.

1. Introduction

The electric currents induced in the modern technological systems generated by geomagnetic storms (known as geomagnetically induced currents or GICs) can disrupt or damage the transformers of the high voltage power grids, or alter the pipe-to-soil voltages in oil or gas pipelines. GICs are associated with geomagnetic disturbances which have a high geomagnetic rate of change in the region of the electricity transport network. Accordingly, such harmful effects have been usually observed only at high geomagnetic latitudes (such as in Canada or Scandinavia), because it is at the regions dominated by the auroral ionospheric currents where the ground magnetic field variation signatures reach the highest amplitudes. Nevertheless, large GICs have been measured at any latitude, even at equatorial locations [*Kappenman*, 2003] and some transformer failures were even reported in South Africa on the occasion of the Halloween storms of 2003 [*Gaunt and Coetzee*, 2007]. *Kappenman* [2005] argued that the source of sustained GICs at low and middle latitudes are linked with high rates of variation associated with impulsive increases in the solar wind dynamic pressure or ring current intensifications. These facts have encouraged several research groups and agencies to initiate vulnerability assessment studies on power grids or pipelines located at regions previously considered to have low GIC-risk other than South Africa, such as China [*Liu et al.,* 2009], Japan [*Watari et al.*, 2009], Czech Republic [*Hejda and Bochníček*, 2005], Kazakhstan [*Vodyannikov et al.*, 2006], Australia [Marshall *et al.*, 2011] or Brasil [*Trivedi et al.,* 2007]. We were similarly motivated to perform such an analysis in a power grid of northeastern Spain, where we are settled. Despite this recent global enthusiasm, there is still very little published works in Southern Europe and, to our knowledge, this is the first attempt to study and measure GICs in Spain.

Citation: Torta, J. M., L. Serrano, J. R. Regué, A. M. Sánchez, and E. Roldán (2012), Geomagnetically induced currents in a power grid of northeastern Spain, Space Weather, 10, S06002, doi:10.1029/2012SW000793. To view the published open abstract, go to http://dx.doi.org and enter the DOI.

Since the generated geoelectric field not only is dependent on the characteristics of the magnetospheric-ionospheric electric currents, but also on the particular ground conductivity structure, we were tempted to start by comparing the horizontal field records of Ebro (EBR, 40.82ºN, 0.49ºE) and Hermanus (HER, 34.42ºS, 19.22ºE) geomagnetic observatories during the storms of 29-31 October 2003. These records can be taken as representative for the derivation of the induced geoelectric fields in North-Eastern Spain and South Africa, respectively. The geomagnetic latitudes of both observatories, derived relative to the centered geomagnetic dipole computed from the IGRF model at the epoch 2010.0 [*Finlay et al.*, 2011], are significantly different: 43º.1N and 34.1ºS, respectively. Accordingly, it can be seen from Figure 1 that the extreme geomagnetic field disturbances and their rates of change (simply evaluated by their first time-derivative) were larger in EBR than in HER. However, to compare the observations at one station and another it might be more convenient to refer them to a coordinate system that accounts for the departures of geomagnetic field lines from a pure dipole, such as the corrected geomagnetic coordinates (CGM) [*Gustafsson et al.*, 1992]. Since the non-dipole terms of the magnetic field are particularly important in the vicinity of the South Atlantic Ocean, CGM latitudes of EBR and HER (33.7ºN and 42.5ºS, respectively) interchange their relative positions with respect to the traditional geomagnetic coordinates. This is not surprising, since different phases of geomagnetic storms are responses to different physical processes [*Gonzalez et al.*, 1994], which are best organized in different coordinate systems. Hemispherical asymmetries should also play a role. In any case, both observatories are settled in similar mid-latitudinal sectors and record comparable geomagnetic horizontal field changes.

How the geomagnetic induction processes derived from those changes affect the particular high-voltage power transmission systems not only is dependent on the local geological

Citation: Torta, J. M., L. Serrano, J. R. Regué, A. M. Sánchez, and E. Roldán (2012), Geomagnetically induced currents in a power grid of northeastern Spain, Space Weather, 10, S06002, doi:10.1029/2012SW000793. To view the published open abstract, go to http://dx.doi.org and enter the DOI.

conditions, but also on the topology and the electrical characteristics of both the power grid and the transformers of the system. In the attempt to quantitatively assess the GIC threat to the ENDESA power system infrastructures in northeastern Spain, we will first analyze the largest rate-of-changes recorded at EBR, then we will describe the modeling approach used to estimate the GICs induced in the grid on the occasion of the extreme events, and at last we will validate the results by comparing the recently modeled and measured GICs at one of the transformer neutrals of the grid.

2. The largest geomagnetic rate-of-change at Ebro

To infer the degree of vulnerability of terrestrial technological systems against a hypothetical extreme geomagnetic storm event, it is natural to resort to the most severe historical events ever recorded. It is generally accepted that the solar-terrestrial disturbance of September 1859, known as the Carrington event (in honor of its discoverer), not only was the first related event associated with space weather, but also the greatest of them. This was reinforced by the work of *Tsurutani et al.* [2003], who, after reanalyzing the horizontal intensity of the magnetograms of Colaba (the only observatory that continuously recorded the storm of September 2, 1859), concluded that it was consistent with a *Dst* index of -1760 nT, although this was later revised, and reduced by a factor of two to -850 nT [*Siscoe et al.*, 2006, *Riley*, 2012]. It is, in any case, significantly greater than the -640 nT corresponding to the storm of March 13, 1989, the highest since 1957, the first year from which the *Dst* index is computed.

Nevertheless, *Cliver and Svalgaard* [2005], considering various effects related to solar-terrestrial disturbances (ionospheric disturbances, solar energetic particles, solar wind, geomagnetic storms and auroras), found subsequent events with similar or superior records for each of the effects. The standard index of geomagnetic activity with the longest time span

Citation: Torta, J. M., L. Serrano, J. R. Regué, A. M. Sánchez, and E. Roldán (2012), Geomagnetically induced currents in a power grid of northeastern Spain, Space Weather, 10, S06002, doi:10.1029/2012SW000793. To view the published open abstract, go to http://dx.doi.org and enter the DOI.

is the *aa* index, but it is only available since 1868. Therefore, it is not possible to directly compare the storm of 1859 with following periods of severe activity. Thus, *Cliver and Svalgaard* [2004] produced two tables, one with the 25 largest geomagnetic storms based on the Aa_m* index (which is derived from the *aa*) from 1868 to 1998, and another with the same number of major storms, but based on the *Dst* index reconstructed by *Karinen and Mursula* [2004] from 1932 to 2002.

Except for a period of interruption, after the dismantling of the measuring devices during the Spanish Civil War until the subsequent renewal of the geomagnetic instrumentation in 1942, the Ebro Observatory keeps analog records from 1910 to 2000, and digital measurements (at a rate of one datum per minute) from that year until today. We used the lists of the extreme geomagnetic storms of Table V of *Cliver and Svalgaard* [2004] and, after ruling out those previous to 1910 and those for the period between April 1938 and December 1941 (which unfortunately coincides with one of the highest geomagnetic activity), selected the five storms with the highest peak value of the Aa_m* index. To these five historical records we added those which show peak rates of change of the horizontal intensity equal or larger than 50 nT/min from 1980 onwards, as shown in Table 1. The values in this table prior to the year 2000 might present some uncertainty, as they have been derived from the digitization of photographic records on paper. Other important factors to consider are that those old extreme events often resulted in the record exceeding the width of the paper used for this purpose for a number of hours, or that the high speed of the magnet movements during certain periods of those episodes prevented the photographic paper from being adequately emulsified by the light beams. Unfortunately, it is precisely on these moments of maximum variation within a short period of time that the maximum geoelectric field amplitudes are produced and can be

Citation: Torta, J. M., L. Serrano, J. R. Regué, A. M. Sánchez, and E. Roldán (2012), Geomagnetically induced currents in a power grid of northeastern Spain, Space Weather, 10, S06002, doi:10.1029/2012SW000793. To view the published open abstract, go to http://dx.doi.org and enter the DOI.

induced in the power grid and must therefore be analyzed. Thus, some of the dB_H/dt peak values of Table 1 could be even greater during the course of the corresponding storms.

From Table 1, a conclusion already pointed out by *Kappenman* [2005], can be derived: geomagnetic indices indicate that severe levels of geomagnetic field horizontal intensity (B_H) do not provide direct specific characterization of the ranges of the first derivative of the field (dB_H/dt) that are important to characterize the levels of GICs. The maximum values of dB_H/dt occur obviously at the same time of the major geomagnetic storms (according to the maximum range of variation in the amplitude of B_H), but the periods of maximum variation do not correlate directly with those peak amplitudes. A typical case is given in the storm of 24-25 March 1991, which ranks last in table VI (and it even did not appear in the table V) of *Cliver and Svalgaard* [2004], but it provided a maximum value of dB_H/dt equal to 177 nT/min at EBR and therefore ranks first in our Table 1. This is because, in low and middle latitudes, the maximum values of dB_H/dt often occur coincident with the abrupt onset of the storm and not during its main phase. The case of March 1991 represents a paradigmatic example of one of these events [*Kappenman*, 2003].

3. GIC modeling

To derive the geoelectric field from geomagnetic field variations several strategies can be followed [*Pirjola,* 2002]. The simplest model considers a plane wave primary field that propagates vertically downwards, and the Earth with a uniform conductivity, σ. This simple model has been shown to be a very reasonable approach for GIC computation when the geomagnetic field variations are obtained sufficiently close to the location where GIC is computed and the characteristics of the source currents are fairly uniform [*Pulkkinen et al.*, 2006], as in our case at a mid-latitudinal region, where the source field is more uniform than

Citation: Torta, J. M., L. Serrano, J. R. Regué, A. M. Sánchez, and E. Roldán (2012), Geomagnetically induced currents in a power grid of northeastern Spain, Space Weather, 10, S06002, doi:10.1029/2012SW000793. To view the published open abstract, go to http://dx.doi.org and enter the DOI.

at the auroral regions. Its efficiency also depends on the gradients of the ground conductivity, but if both the magnetic field variations and GIC are measured and the grid parameters are known, the ”effective” ground conductivity can be solved at a later stage.

Using thus the plane wave model approach, the North and East components of the geoelectric field can be computed in terms of the derivative of the East and North geomagnetic field components, respectively [e.g. *Pirjola,* 2002; *Ngwira et al.*, 2011]:

$$E_{x,y}(t) = \pm \frac{1}{\sqrt{\pi \mu_0 \sigma}} \int_{-\infty}^{t} \frac{1}{\sqrt{t-u}} \frac{dB_{y,x}(u)}{dt} du, \qquad (1)$$

where μ_0 is the permeability of the free space. The values of the electric field are thus dependent of the present and recent values of the geomagnetic field derivative. The integral of equation (1) can be solved numerically [*Viljanen and Pirjola*, 1989] and, accordingly, a value for the integration time has to be chosen. Using EBR data at a sampling rate of 1/min during some significant storms, it was revealed that integrating the magnetic field variations more than 30 min backward in time did not change the derived electric fields.

We are not aware of the existence of an integrated conductivity model valid for our region of interest. Based on a model of electrical resistivity from magnetotelluric measurements, which includes a NS profile from the Pyrenees to near the Mediterranean coast along about the meridian 1º E [*Pous et al.,* 1995], it can be observed that it varies strongly with depth and, specially, below a depth of 30 km, with the latitude as well. Due to the relatively low frequency of the phenomena under concern, small-scale conductivity anomalies near the surface are not important when calculating the geoelectric field that causes the GIC, as these fields penetrate to a certain depth. According to the *Pous et al.* [1995] model, we can distinguish three significant layers. The first one extends to 30 km depth and presents a fairly

Citation: Torta, J. M., L. Serrano, J. R. Regué, A. M. Sánchez, and E. Roldán (2012), Geomagnetically induced currents in a power grid of northeastern Spain, Space Weather, 10, S06002, doi:10.1029/2012SW000793. To view the published open abstract, go to http://dx.doi.org and enter the DOI.

homogeneous resistivity of more than 3000 Ωm (conductivity below 0.0003 S/m). Below this layer and to a 80-km depth, another layer with resistivity of about 1000 Ωm (σ = 0.001 S/m) is found at the Pyrenees (on the North) and the Ebro Valley (on the South), while the central part of the territory is less resistive (more conductive) at this intermediate layer, with values ranging from 1 Ωm (σ = 1 S/m) to 30 Ωm (σ = 0.03 S/m). The bottom layer (resolved to a depth of 120 km) is still resistive (σ =0.001 S/m) below the Pyrenees and relatively conductive on the rest (σ =0.3-0.1 S/m). Thus, a value of σ = 0.001 S/m turned out to be a reasonable assumption for the effective homogeneous conductivity of our initial model.

Figure 2 shows the E_x and E_y components of the geoelectric field as derived trough the plane wave model and parameters described above during the storm of October 29-31, 2003 with EBR geomagnetic field data. Note that sometimes the EW electric field is larger, while at other times the NS electric field is larger. This storm event corresponds to a clear example of source of relatively large sustained geoelectric field amplitudes, which are capable of producing measurable GICs in the power grids. Storms with intense, sudden commencements produced even larger peaks (Ey = -0.73 V/km for that of March 24, 1991) but for brief periods of time during those events, which are associated to magnetospheric shocks related to impulsive increases in solar wind dynamic pressure.

As regards the method for calculating the currents in the earthed conductor network, we used the approach of *Lehtinen and Pirjola* [1985], which is based on Ohm's and Kirchoff's laws. The model assumes that the induced currents are generated from a known external electric field (1) acting on the electrical circuit. Both the electric field and currents are considered time-independent because geomagnetic variations have frequencies significantly below the 50

Citation: Torta, J. M., L. Serrano, J. R. Regué, A. M. Sánchez, and E. Roldán (2012), Geomagnetically induced currents in a power grid of northeastern Spain, Space Weather, 10, S06002, doi:10.1029/2012SW000793. To view the published open abstract, go to http://dx.doi.org and enter the DOI.

Hz mains. At each node (earthing point in a transformer) the GIC (with positive direction assumed to be into earth) is given as the elements of the following vector:

$$\mathbf{I} = (1 + \mathbf{YZ})^{-1}\,\mathbf{J}, \tag{2}$$

where **Y** and **Z** are the network admittance and earthing impedance matrices, respectively and the matrix **J** involves the voltages obtained by integrating the geoelectric field along the paths defined by the transmission lines in the power grid [*Pulkkinen et al.*, 2006; *Wik et al.,* 2008]. Assuming that the nodes are sufficiently far apart, the impedance matrix is a diagonal matrix whose elements are the ground resistances at each node, while the admittance matrix contains the inverse values of the resistances of the high-voltage lines between connected nodes. To calculate the earthing resistances the power company provided us the necessary information about the number of transformers (with the neutral grounded) in each station and their configuration. Of each transformer we needed to know all resistive parameters, i.e. the resistance of its windings and of its reactors, if any, and the grounding resistances.

Considering that the electric field is spatially constant in the region of analysis, the GIC can be decomposed into two components, one related to the North direction of the electric field and the other to its East direction [*Viljanen and Pirjola*, 1994]:

$$GIC(t) = aE_x(t) + bE_y(t). \tag{3}$$

a and *b* are known as the network constants in each node and their units are [A km / V]. They are obtained from equation (2) by applying a constant field of 1 V/km northwards, and eastwards, respectively. The values of these constants depend on the resistive parameters of the power lines and of the transformers and their topology in the substations, and of the orientation of the power lines. High values of *a* and *b* indicate that the substation is prone to experience large GICs.

Citation: Torta, J. M., L. Serrano, J. R. Regué, A. M. Sánchez, and E. Roldán (2012), Geomagnetically induced currents in a power grid of northeastern Spain, Space Weather, 10, S06002, doi:10.1029/2012SW000793. To view the published open abstract, go to http://dx.doi.org and enter the DOI.

Our initial model considered only the 400 kV network of the Northeasternmost Spanish grid, including 17 nodes and 23 lines (some of them doubled) (Figure 3). In many cases the substations are composed of several transformers, and the total GIC flowing in the node is shared among their neutrals. In order to determine the individual affectation at each transformer we defined the constants a_t and b_t, which are derived from the constants a and b using the corresponding current divider, which depends on the equivalent resistance of each transformer and the total equivalent resistance of the node. To calculate the total ground resistance we considered the three phases in parallel and added the earthing resistance. If the substation is composed of more than one transformer, we assumed that the transformers are connected in parallel and share the same earthing resistance. At some substations the 400 kV network is connected to the 220 kV system by autotransformers. In these cases we ignored completely the low voltage sides of the circuit, and took the total resistance of the winding as the resistance of the transformer.

Changes in the power grid configuration occur every now and then, so that some resistances in earthing leads of transformer neutrals or some transmission lines must be excluded from the power grid model on the occasion of some events. For a geomagnetic storm occurred on October 24-25, 2011 our model provided the values of Table 2. In such occasion, the lines Ascó-Pierola, Vandellòs-Pierola and Vandellòs-Rubí were disconnected. Also, the entire grid should be modeled, but only a smaller part has been considered, so some border substations reflected the highest GIC levels due to the fact that the current from the rest of the grid is forced to flow only to a single point (at particular times), so values at those border stations are not considered real and consequently are not shown. The table highlights the transformers most vulnerable to GICs, i.e. those which show the largest b_t values, although depending on the morphology of the induced field, other transformers could be prone to experience larger

Citation: Torta, J. M., L. Serrano, J. R. Regué, A. M. Sánchez, and E. Roldán (2012), Geomagnetically induced currents in a power grid of northeastern Spain, Space Weather, 10, S06002, doi:10.1029/2012SW000793. To view the published open abstract, go to http://dx.doi.org and enter the DOI.

GICs on the occasion of large E_x fields, i.e. those associated with the largest a_t values. Using the corresponding a_t and b_t values, the GICs that the storm of 24 March 1991 (the one with the highest peak of dB_H/dt recorded at EBR) produced at one of those most vulnerable transformer would had been those shown in Figure 4. Other transformers (at the substations with the largest a and/or b values) might experience even much larger GICs on occasions in which some of the rest of transformers in the substation would be disconnected.

4. GIC measurement

In order to know the true effect of GICs in the neutral points of the power grid, a measurement system has been developed and the first prototype placed in one of the transformers. Though not one of the most vulnerable transformers, by logistic reasons the TR2 transformer of Vandellòs substation was selected for the measurement of the actual GIC flowing through its neutral. The block diagram of the measurement system is shown in Figure 5. By means of an open-loop Hall-effect transducer and a Real-Time Acquisition System, the current flowing through the neutral is measured, digitized at the sampling frequency of 1 kHz, and synchronized via the Global Positioning System (GPS) time information, obtained from a GPS antenna. Temperature variations of the measurement system are also measured by means of thermocouples in order to apply temperature corrections on the transducer measurements. The stored information is daily transferred to a local server using the Universal Mobile Telecommunications System (UMTS) connection and automatically processed. By applying the fast Fourier transform (FFT), each minute is analyzed in the frequency domain. This time interval is considered in order to coincide with the sampling time of the geomagnetic data provided by Ebro Observatory. The 1-kHz sampling frequency used by the measurement system not only allows the measurement of the GIC (actually measured as a DC current in a one-minute time interval), but it also measures the 50-Hz current present in the neutral due to

Citation: Torta, J. M., L. Serrano, J. R. Regué, A. M. Sánchez, and E. Roldán (2012), Geomagnetically induced currents in a power grid of northeastern Spain, Space Weather, 10, S06002, doi:10.1029/2012SW000793. To view the published open abstract, go to http://dx.doi.org and enter the DOI.

imbalances in the power grid and/or in the transformer. In case of 50-Hz half cycle saturation, spectral information up to the tenth harmonic can be examined. This is essential to know the saturation level of the transformer core induced by the GIC and, if needed, to prevent a possible thermal damage. Therefore, the minute time course of the amplitudes of the GIC, the 50-Hz current and its harmonics can be analyzed and, in the GIC case, compared to the ones predicted by the model presented before.

Our preliminary model results at Vandellòs were not in principle in agreement with the measured GIC at this substation, but they became (see Figure 6) in satisfactory agreement (linear correlation coefficient of 0.77) when we changed the Earth's conductivity to a value of 0.0001 S/m. This is an aspect that needs further investigation.

Assuming that the electric field is spatially uniform, those a_t and b_t values can be also obtained empirically for this specific GIC site using 2880 samples from recent measurements taken with the above described device at Vandellòs substation during October 24-25, 2011. We will then substitute a_t and b_t by α_t and β_t and write [*Wik et al.*, 2008]:

$$GIC(t) = \alpha_t E_x(t) + \beta_t E_y(t). \tag{4}$$

According to *Pulkkinen et al.* [2007] the empirical system parameters can be determined as:

$$\alpha_t = \frac{\langle \mathrm{GIC\,E_y} \rangle \langle \mathrm{E_x E_y} \rangle - \langle \mathrm{GIC\,E_x} \rangle \langle \mathrm{E_y^2} \rangle}{\langle \mathrm{E_x E_y} \rangle^2 - \langle \mathrm{E_x^2} \rangle \langle \mathrm{E_y^2} \rangle} \tag{5}$$

$$\beta_t = \frac{\langle \mathrm{GIC\,E_x} \rangle \langle \mathrm{E_x E_y} \rangle - \langle \mathrm{GIC\,E_y} \rangle \langle \mathrm{E_x^2} \rangle}{\langle \mathrm{E_x E_y} \rangle^2 - \langle \mathrm{E_x^2} \rangle \langle \mathrm{E_y^2} \rangle}, \tag{6}$$

where $< \cdot >$ denotes the expectation taken over different realizations of the process. Accordingly, the obtained values were α_t=-3.57 and β_t= 4.22 A km / V, which certainly differ from the corresponding a_t and b_t of the TR2 transformer of Vandellòs of Table 2. The ratio

Citation: Torta, J. M., L. Serrano, J. R. Regué, A. M. Sánchez, and E. Roldán (2012), Geomagnetically induced currents in a power grid of northeastern Spain, Space Weather, 10, S06002, doi:10.1029/2012SW000793. To view the published open abstract, go to http://dx.doi.org and enter the DOI.

$c_t = \beta_t / \alpha_t$ is equal to -1.18. This ratio can be obtained directly from the measured ground geomagnetic variations [*Pulkkinen et al.*, 2007]:

$$c'_t = \frac{\langle \mathrm{B_y B_x} \rangle - \chi \langle \mathrm{B_y\ B_y} \rangle}{\langle \mathrm{B_x B_x} \rangle - \chi \langle \mathrm{B_x\ B_y} \rangle}, \quad (7)$$

where

$$\chi = \frac{\langle \mathrm{GIC\ B_x} \rangle}{\langle \mathrm{GIC\ B_y} \rangle}, \quad (8)$$

In this way c'_t= -1.03, which is very similar to c_t. Since the way in which this latter value is obtained is independent of the electric field, this result validates the assumptions that we adopted to derive it.

Using those latter constant values we calculated GIC at the TR2 transformer of Vandellòs for the recent event of October 2011 and compared them with the measured ones (Figure 7). The modeled GIC by means of independently obtained empirical parameters is in good agreement with the measured GIC (linear correlation coefficient of 0.87).

5. Discussion

To what extent is the extreme event of 1859 or are those registered in 1991, 1921, 2000, 1982 or 1989 representative for evaluating the major risk from a geomagnetic storm in our latitudes? In their conclusions *Cliver and Svalgaard* [2004] indicated that solar active regions significantly higher than the large and complex region (sunspot area ~ 2300 millionths of a hemisphere) that originated in the flare of September, 1 1859 have been observed. Therefore, future events might exceed any or all of the magnitudes of the most extreme reported phenomena. Recently, *Vasyliūnas* [2010], based on physical reasoning, has estimated that the upper limit of the *Dst* index for the eventual biggest geomagnetic storm that might occur is ~ -

Citation: Torta, J. M., L. Serrano, J. R. Regué, A. M. Sánchez, and E. Roldán (2012), Geomagnetically induced currents in a power grid of northeastern Spain, Space Weather, 10, S06002, doi:10.1029/2012SW000793. To view the published open abstract, go to http://dx.doi.org and enter the DOI.

2500 nT, 30% higher than the largest assumed value of -1760 nT assigned to the Carrington event of 1859.

However, as already mentioned, GICs are associated with geomagnetic disturbances which have a high rate of change in the region where the electricity transport network is located, while geomagnetic indices only account for the maximum amplitude variation on a global level. It is more difficult to estimate the largest imaginable rate of variation in a regional basis. It can be characterized only by the morphology of the already recorded storms in the vicinity of each infrastructure (e.g., at Ebro Observatory for the North-Eastern Spanish power grid) and assume that new periods of high activity will be reasonably comparable. Recent initiatives [Thomson et al., 2011, Pulkkinen et al., 2012] use extreme value statistics to explore the variations that might be observed every 100 or 200 years, but it has to be taken into account that only one decade of digital magnetic data falls far short of the required duration to provide robust assessments even of the 1-in-100 years risk.

Our forensic analysis revealed that the largest magnitude of the horizontal component of the geomagnetic field change per minute at EBR, which keep archives since 1910, reached an intensity of at least 177 nT/min (a definitive confirmation is not possible with the limitations of the old paper chart archives). This empirical upper limit is much lower than the intensities that triggered power system impacts at higher latitude regions, such as the Quebec grid blackout during the March 1989 storm (which was of 479 nT/min), although other power grid impacts of importance have been observed at levels lower than 100 nT/min [*Kappenman*, 2006].

Citation: Torta, J. M., L. Serrano, J. R. Regué, A. M. Sánchez, and E. Roldán (2012), Geomagnetically induced currents in a power grid of northeastern Spain, Space Weather, 10, S06002, doi:10.1029/2012SW000793. To view the published open abstract, go to http://dx.doi.org and enter the DOI.

In addition to this assessment of the expected worst case scenario, research was initiated to, on one hand, calculate the GICs expected throughout the NorthEastern Spanish grid to identify substations and transformers potentially most susceptible to damage and, on the other hand, monitor GICs at one particular transformer neutral to provide measurements for verification of the calculations. Although the assumed plane wave approach to the calculation may not be accurate, and the actual ground conductivity might differ from the assumed value of 0.001 S/m locally, our initial results confirm the validity of the method used to derive the geoelectric field. There is also a need for the knowledge of the electrical (near-DC) characteristics of the grid changes over time.

Since Ebro observatory is placed within the region of the grid network we were studying, the uniform plane wave method has been completely adequate for our initial investigations, and much simpler. Some of the foreseen improvements when we will move to model the entire Spanish grid rely on the modeling of the magnetic fields with spherical elementary currents systems (SECS), a technique of interpolation introduced by *Amm* [1997]. The recordings at the other two geomagnetic observatories in the Spanish Mainland, and possibly those from the neighboring countries will then also be used. GIC data, together with geomagnetic observatory data will be used in order to obtain a multilayered ground conductivity structure, which might, in turn, improve the modeling results.

Acknowledgments

This research is part of the project "Prediction and monitoring of geomagnetically induced currents in the ENDESA system and risks assessment", funded by ENDESA Distribución Eléctrica, S.L. The authors are grateful to an anonymous referee for his useful comments which helped to improve the manuscript.

References

Amm, O. (1997), Ionospheric elementary current systems in spherical coordinates and their application, *J. Geomagnetism Geoelectricity*, 49, 947–955.

Cliver, E.W. and L. Svalgaard (2004), The 1859 Solar-Terrestrial Disturbance and the Current Limits of Extreme Space Weather Activity, *Solar Physics, 224*, 407-422.

Finlay. C. C., et al. (2010), International Geomagnetic Reference Field: the eleventh generation, *Geophys. J. Int., 183*, 1216–1230.

Gaunt, C. T., and G. Coetzee (2007), Transformer failure in regions incorrectly considered to have low GIC-risk, paper presented at Power Tech 2007, Inst. of Electr. and Electron. Eng., Lausanne, Switzerland.

Gonzalez, W.D., J.A. Joselyn, Y. Kamide, H.W. Kroehl, G. Rostoker, B.T. Tsurutani, V.M. Vasyliunas (1994), What is a geomagnetic storm? *Journal of Geophysical Research, 99*, 5771-5792.

Gustafsson, G., N. E. Papitashvili, and V. O. Papitashvili (1992), A Revised Corrected Geomagnetic Coordinate System for Epochs 1985 and 1990, *J. Atmos. Terr. Phys.*, *54*, 1609-1631.

Hejda, P. and J. Bochníček (2005), Geomagnetically induced pipe-to-soil voltages in the Czech oil pipelines during October-November 2003, *Ann. Geophys., 23*, 3089–3093.

Kappenman, J. G. (2003), Storm sudden commencement events and the associated geomagnetically induced current risks to ground-based systems at low-latitude and mid-latitude locations, *Space Weather, 1(3)*, 1016, doi:10.1029/2003SW000009.

Kappenman, J.G. (2005), An overview of the impulsive geomagnetic field disturbances and power grid impacts associated with the violent Sun–Earth connection events of 29–31 October 2003 and a comparative evaluation with other contemporary storms. *Space Weather, 3*, S08C01 doi: 10.1029/2004SW000128.

Kappenman, J.G. (2006), Great geomagnetic storms and extreme impulsive geomagnetic field disturbance events – An analysis of observational evidence including the great storm of May 1921, *Advances in Space Research, 38*, 188–199.

Karinen, A. and Mursula, K. (2005), A new reconstruction of the Dst index for 1932–2002, *Ann. Geophysicae, 23*, 475–485.

Lehtinen, M., R. Pirjola (1985), Currents produced in earthed conductor networks by geomagnetically-induced electric fields. *Annales Geophysicae, 3(4)*, 479-484.

Citation: Torta, J. M., L. Serrano, J. R. Regué, A. M. Sánchez, and E. Roldán (2012), Geomagnetically induced currents in a power grid of northeastern Spain, Space Weather, 10, S06002, doi:10.1029/2012SW000793. To view the published open abstract, go to http://dx.doi.org and enter the DOI.

Liu, C.-M., L.-G. Liu, R. Pirjola, and Z.-Z. Wang (2009), Calculation of geomagnetically induced currents in mid to low-latitude power grids based on the plane wave method: a preliminary case study. *Space Weather, 7*, S04005, doi:10.1029/2008SW000439.

Marshall, R. A., E. A. Smith, M. J. Francis, C. L. Waters, and M. D. Sciffer (2011), A Preliminary Risk Assessment of the Australian region Power Network to Space Weather, *Space Weather*, 9, S10004, doi:10.1029/2011SW000685.

Ngwira, M., L.A. McKinnell, and P. J. Cilliers (2011), Geomagnetic activity indicators for geomagnetically induced current studies in South Africa, *Advances in Space Research, 48*, 529–534.

Pirjola, R. (2002), Review on the calculation of surface electric and magnetic fields and of geomagnetically induced currents in ground-based technological systems, *Surveys in Geophysics, 23*, 71-90.

Pous, J., J. Ledo, A. Marcuello, and M. Daignières (1995), Electrical resistivity model of the crust and upper mantle from a magnetotelluric survey through the central Pyrenees. *Geophys. J. Int., 121(3)*, 750–762.

Pulkkinen, A., A. Viljanen, and R. Pirjola (2006), Estimation of geomagnetically induced current levels from different input data, *Space Weather*, 4, S08005, doi:10.1029/2006SW000229.

Pulkkinen, A., R. Pirjola, and A. Viljanen (2007), Determination of ground conductivity and system parameters for optimal modeling of geomagnetically induced current flow in technological systems, *Earth, Planets and Space,* 59, 999–1006.

Pulkkinen, A., E. Bernabeu, J. Eichner, C. Beggan, and A. Thomson (2012), Generation of 100-year geomagnetically induced current scenarios, *Space Weather* (in press).

Riley, P. (2012), On the probability of occurrence of extreme space weather events, *Space Weather*, 10, S02012, doi: 10.1029/2011SW000734.

Siscoe, G., N. U. Crooker, and C. R. Clauer (2006), Dst of the Carrington storm of 1859, *Adv. Space Res.*, 38, 173–179, doi:10.1016/j.asr.2005.02.102.

Thomson, A., S. Reay, and E. Dawson (2011), Quantifying Extreme Behaviour in Geomagnetic Activity, *Space Weather*, 9, S10001, doi: 10.1029/2011SW000696.

Trivedi, N.B., et al. (2007), Geomagnetically induced currents in an electric power transmission system at low latitudes in Brazil: A case study, *Space Weather*, *5*, S04004, doi: 10.1029/2006SW000282.

Citation: Torta, J. M., L. Serrano, J. R. Regué, A. M. Sánchez, and E. Roldán (2012), Geomagnetically induced currents in a power grid of northeastern Spain, Space Weather, 10, S06002, doi:10.1029/2012SW000793. To view the published open abstract, go to http://dx.doi.org and enter the DOI.

Tsurutani, B. T., Gonzalez, W. D., Lakhina, G. S., and Alex, S. (2003), The extreme magnetic storm of 1-2 September 1859, *J. Geophys. Res., 108*, No. A7, 1268, doi:10.1029/2002JA009504.

Vasyliūnas, V.M. (2010), The largest imaginable magnetic storm. *Journal of Atmospheric and Solar-Terrestrial Physics*, doi:10.1016/j.jastp.2010.05.012.

Viljanen, A., and R. Pirjola (1989), Statistics on geomagnetically-induced currents in the Finnish 400 kV power system based on recordings of geomagnetic variations, *J. Geomag. Geoelectr., 41*, 411-420.

Viljanen, A., and R. Pirjola (1994), Geomagnetically induced currents in the Finnish high-voltage power system, *Surveys in Geophysics, 15*, 383-408.

Vodyannikov, V.V., G.I. Gordienko, S.A. Nechaev, O.I. Sokolova, S.J. Homutov, and A.F. Yakovets (2006), Geomagnetically induced currents in power lines according to data on geomagnetic variations, *Geomagnetism and Aeronomy, 46*, 809-813.

Watari, S., M. Kunitake, K. Kitamura, T. Hori, T. Kikuchi, K. Shiokawa, N. Nishitani, R. Kataoka, Y. Kamide, T. Aso, Y. Watanabe, and Y. Tsuneta (2009), Measurements of geomagnetically induced current in a power grid in Hokkaido, Japan. *Space Weather, 7*, S03002, doi:10.1029/2008SW000417.

Wik, M., A. Viljanen, R. Pirjola, A. Pulkkinen, P. Wintoft, and H. Lundstedt (2008), Calculation of geomagnetically induced currents in the 400 kV power grid in southern Sweden, *Space Weather*, 6, S07005, doi:10.1029/2007SW000343.

Citation: Torta, J. M., L. Serrano, J. R. Regué, A. M. Sánchez, and E. Roldán (2012), Geomagnetically induced currents in a power grid of northeastern Spain, Space Weather, 10, S06002, doi:10.1029/2012SW000793. To view the published open abstract, go to http://dx.doi.org and enter the DOI.

Figure Captions.

Figure 1. Left: B_H component of the HER (South Africa) magnetic field (top) and time derivative (botttom) during 29-31 October 2003. Right: The same event as recorded at EBR (Spain).

Figure 2. The calculated horizontal electric field at the Earth's surface on 29-31 October 2003 as derived from EBR geomagnetic data.

Figure 3. The North-eastern subset of the Spanish power transmission network, including only the 400 kV elements. The names of the substations and the location of EBR observatory are shown.

Figure 4. GIC at the transformer of Can Jardí substation for the three days starting at 00:00h of March 24, 1991, using the values of Table 2.

Figure 5. Block diagram of the measurement system of the GIC and the 50-Hz current at the neutral of the transformer.

Figure 6. Measured (red) and calculated (blue) GIC at the TR2 transformer of Vandellòs for the event of 24-25 October 2011. The uniform ground conductivity was set to 0.0001 S/m.

Figure 7. Measured (red) and calculated using empirical network constants (blue) GIC at the TR2 transformer of Vandellòs for the event of 24-25 October 2011. The uniform ground conductivity was set to 0.0001 S/m.

Citation: Torta, J. M., L. Serrano, J. R. Regué, A. M. Sánchez, and E. Roldán (2012), Geomagnetically induced currents in a power grid of northeastern Spain, Space Weather, 10, S06002, doi:10.1029/2012SW000793. To view the published open abstract, go to http://dx.doi.org and enter the DOI.

Table 1. Largest rates of change in B_H at EBR

Date			Peak *aa* (nT)	Peak dB_H/dt (nT/min)
24	Mar	1991	363	177
14	May	1921	680	135
15	Jul	2000	440	112
13	Jul	1982	497	110
13	Mar	1989	715	92
29	Oct	2003	715	83
26	Jul	2004	228	82
31	Mar	2001	284	72
28	Mar	1946	656	70
24	Nov	2001	445	69
06	Nov	2001	306	64
05	Jun	1991	363	64
13	Nov	1960	568	55
09	Nov	2004	363	55
08	Nov	1991	578	50
08	Jul	1928	656	50

Citation: Torta, J. M., L. Serrano, J. R. Regué, A. M. Sánchez, and E. Roldán (2012), Geomagnetically induced currents in a power grid of northeastern Spain, Space Weather, 10, S06002, doi:10.1029/2012SW000793. To view the published open abstract, go to http://dx.doi.org and enter the DOI.

Table 2. The obtained network constants at each substation. *a* is the value for an eastward electric field of 1 V/km and *b* that for a northern electric field of E_x = 1 V/km. Note that some substations have several transformers, so that the given GIC must be divided between them, and the corresponding constants for each transformer are then a_t and b_t.

Station	Number of transformers	Transformer	*a*	*b*	*at*	*bt*
		TG1			1.22	-34.51
Ascó	3	TG2	2.87	-81.14	1.22	-34.51
		TR3			0.43	-12.12
Begues	2	ATR3	-9.07	59.57	-4.53	29.78
		ATR4			-4.53	29.78
Calders	1	TR1	12.46	26.22	12.46	26.22
Can Barba	1	TR6	-16.62	51.81	-8.31	25.91
		TR7			-8.31	25.91
Can Jardí	1	ATR4	12.80	44.85	12.80	44.85
Garraf	1	TR1	-11.29	26.02	-11.29	26.02
Mequinenza	1	ATR2	6.86	-26.76	6.86	-26.76
Pierola	2	TR1	-45.60	-22.79	-22.61	-11.30
		ATR4			-22.99	-11.49
Plana del vent	2	TG1	-31.78	4.54	-15.89	2.27
		TG2			-15.89	2.27
Rubí	2	ATR7	19.33	64.96	10.20	34.29
		ATR8			9.13	30.67
		TG1			21.54	-16.34
Sallente	4	TG2	83.90	-63.63	21.20	-16.08
		TG3			20.63	-15.65
		TG4			20.52	-15.57
		ATR2			3.12	33.72
Sentmenat	3	ATR3	9.52	102.88	3.34	36.07
		ATR4			3.06	33.09
		TR1			-5.76	1.61
Vandellòs	3	TR2	-25.57	7.14	-6.92	1.93
		TG1			-12.89	3.60
		ATR1			-1.01	0.27
Vic	4	ATR2	-8.45	2.22	-1.25	0.33
		ATR3			-1.25	0.33
		ATR4			-4.95	1.30

Citation: Torta, J. M., L. Serrano, J. R. Regué, A. M. Sánchez, and E. Roldán (2012), Geomagnetically induced currents in a power grid of northeastern Spain, Space Weather, 10, S06002, doi:10.1029/2012SW000793. To view the published open abstract, go to http://dx.doi.org and enter the DOI.

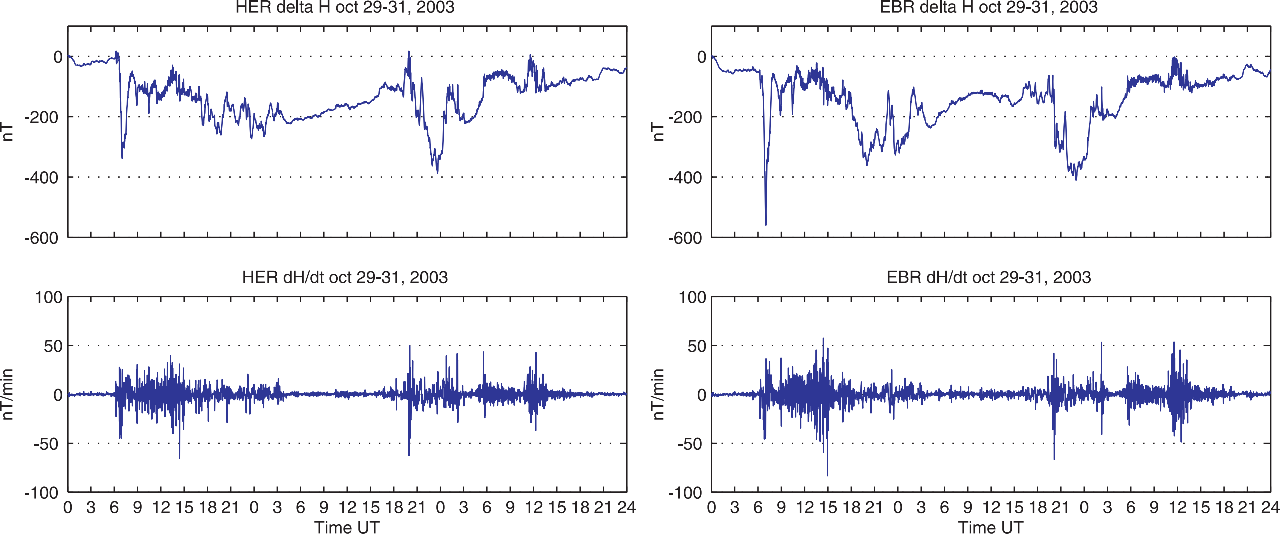
HER delta H oct 29-31, 2003
EBR delta H oct 29-31, 2003
HER dH/dt oct 29-31, 2003
EBR dH/dt oct 29-31, 2003
nT
nT/min
0
-200
-400
-600
100
50
-50
-100
0 3 6 9 12 15 18 21 0 3 6 9 12 15 18 21 0 3 6 9 12 15 18 21 24
Time UT

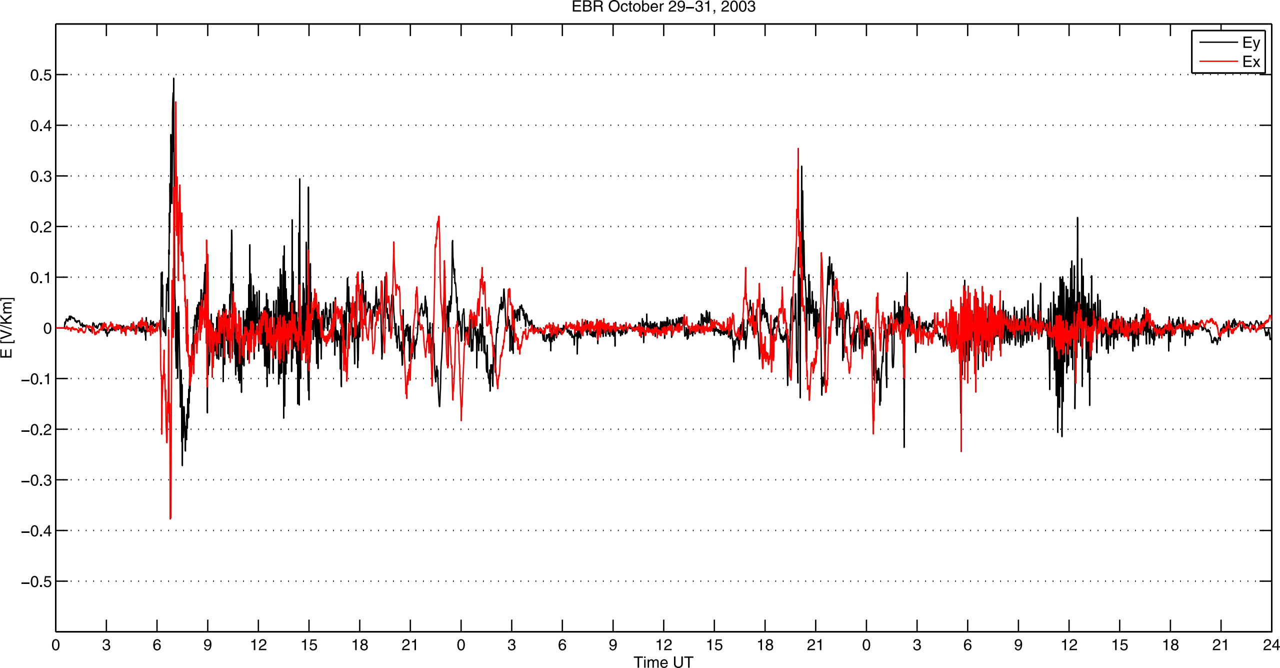

EBR October 29–31, 2003
Ey
Ex
0.5
0.4
0.3
0.2
0.1
0
−0.1
−0.2
−0.3
−0.4
−0.5
E [V/Km]
0 3 6 9 12 15 18 21 0 3 6 9 12 15 18 21 0 3 6 9 12 15 18 21 24
Time UT

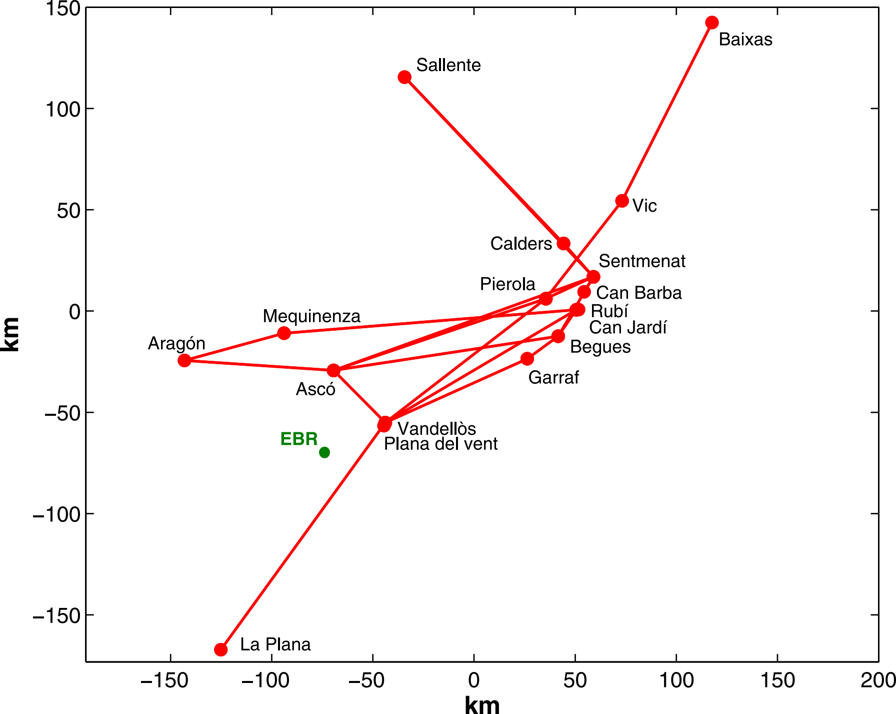

Baixas
Sallente
Vic
Calders
Sentmenat
Pierola
Can Barba
Rubí
Can Jardí
Begues
Mequinenza
Aragón
Ascó
Garraf
Vandellòs
Plana del vent
EBR
La Plana
km
km
150
100
50
0
−50
−100
−150
−150
−100
−50
0
50
100
150
200

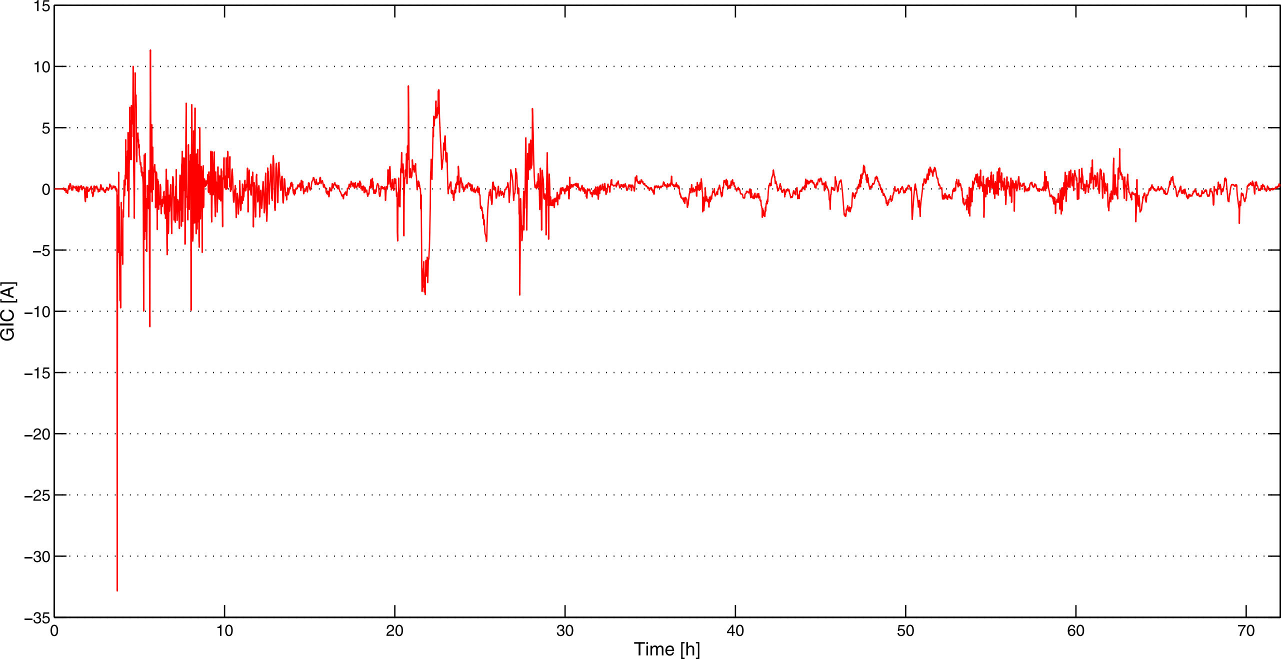
GIC [A]
Time [h]
15
10
5
0
−5
−10
−15
−20
−25
−30
−35
0
10
20
30
40
50
60
70

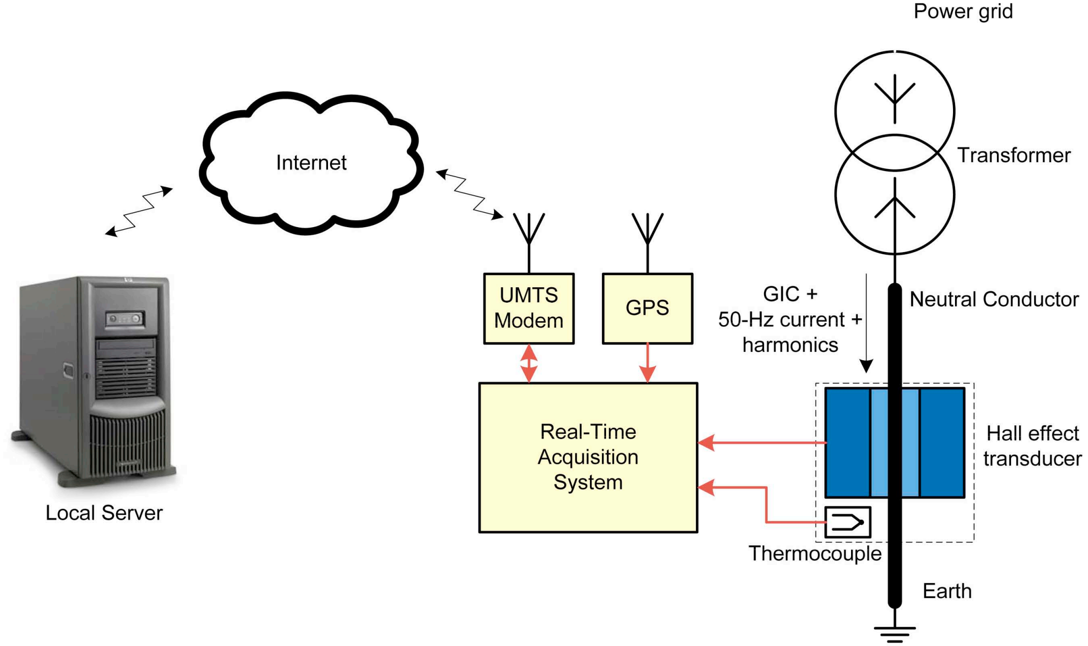
Power grid
Internet
Transformer
Neutral Conductor
GIC +
50-Hz current +
harmonics
UMTS
Modem
GPS
Real-Time
Acquisition
System
Hall effect
transducer
Local Server
Thermocouple
Earth

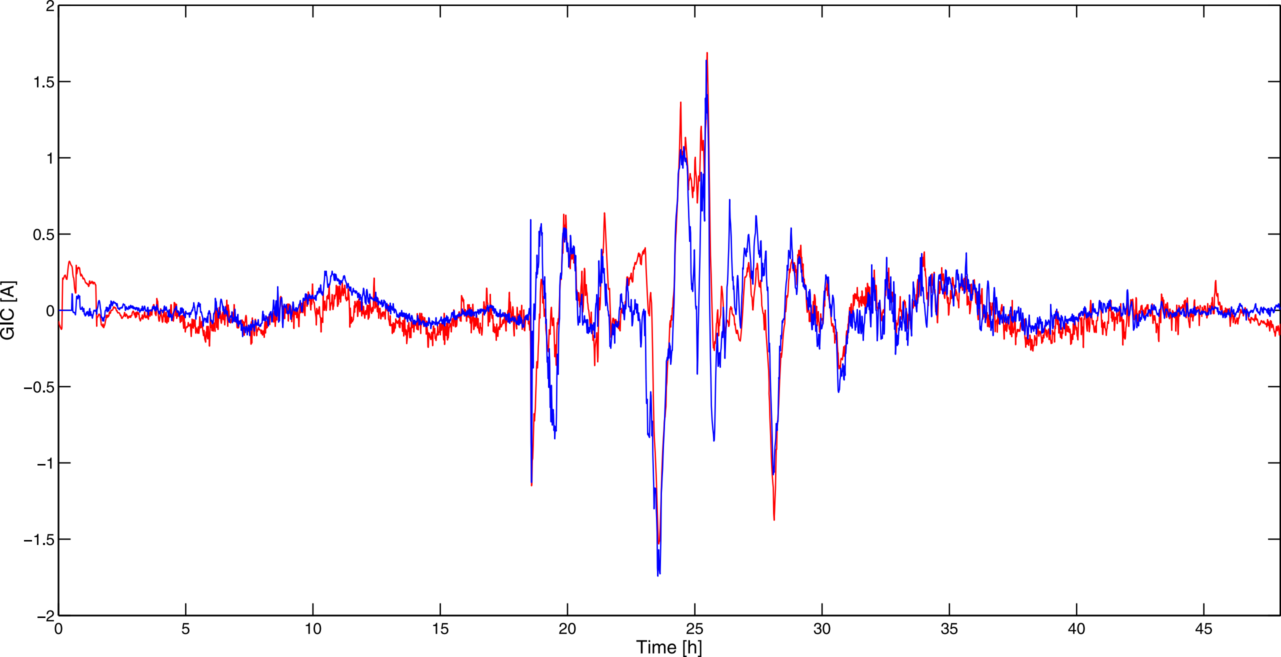
GIC [A]
Time [h]
2
1.5
1
0.5
0
−0.5
−1
−1.5
−2
0
5
10
15
20
25
30
35
40
45

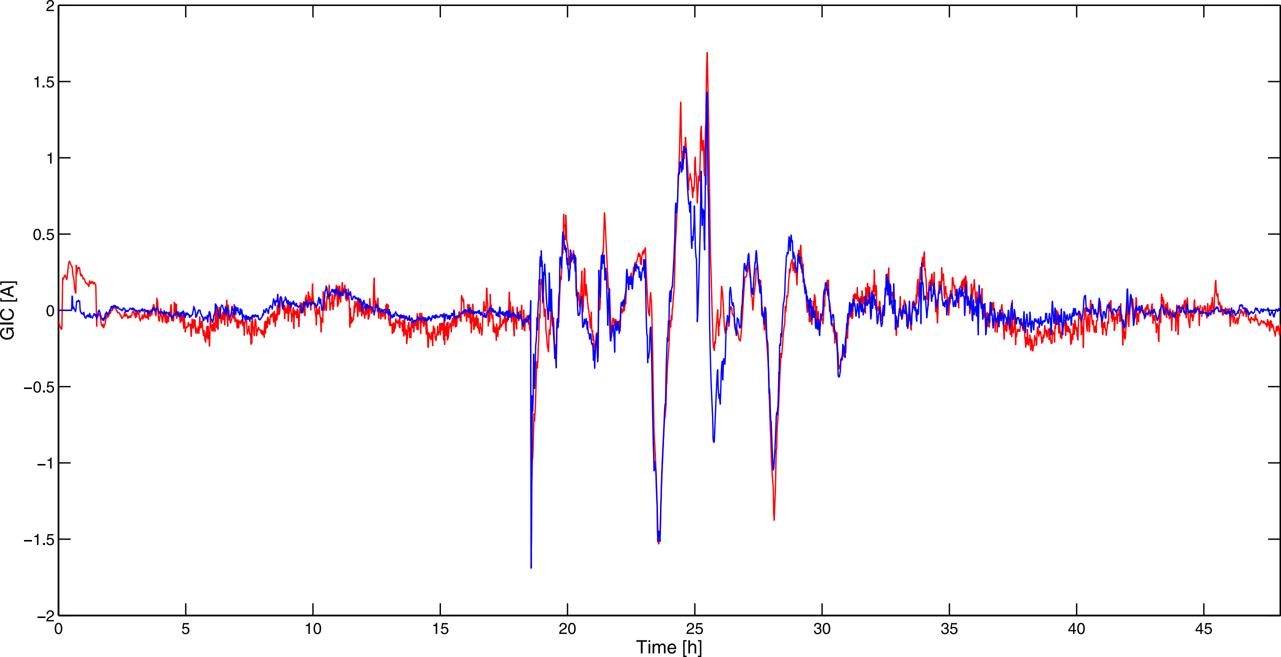

GIC [A]
Time [h]
2
1.5
1
0.5
0
−0.5
−1
−1.5
−2
0
5
10
15
20
25
30
35
40
45